Sheffield Hallam University

Long-term behaviour of Nb and Cr nitrides nanostructured coatings under steam at 650°C. Mechanistic considerations.

AGUERO, A, LORENZA, M.Juez, HOVSEPIAN, Papken
<http://orcid.org/0000-0002-1047-0407>, EHIASARIAN, Arutiun
<http://orcid.org/0000-0001-6080-3946>, PURANDARE, Yashodhan
<http://orcid.org/0000-0002-7544-9027> and MUELAS, R

Available from Sheffield Hallam University Research Archive (SHURA) at:

http://shura.shu.ac.uk/18377/

This document is the author deposited version. You are advised to consult the publisher's version if you wish to cite from it.

Published version

Repository use policy

Long-term behaviour of Nb and Cr nitrides nanostructured coatings under steam at 650°C. Mechanistic considerations.

A. Agüero[1*], M. Juez-Lorenzo[2], P. Eh. Hovsepian[3], A.P. Ehiasarian[3], Y.P. Purandare[3] and R. Muelas[4].

[1]Instituto Nacional de Técnica Aeroespacial (INTA), Ctra. Ajalvir Km. 4, 28850 Torrejón de Ardoz (Madrid), Spain

[2] Fraunhofer Institut für Chemische Technologie ICT, Joseph-von-Fraunhofer-Straße 7, 76327 Pfinztal, Germany

[3] National HIPIMS Technology Centre, Materials and Engineering Research Institute, Howard Street, Sheffield Hallam University, Sheffield, S1 1WB, UK.

[4]Ingeniería de Sistemas para la Defensa de España SA, Beatriz de Bobadilla No. 3, Madrid, 28040 Spain

* Corresponding author: Email: agueroba@inta.es.

Abstract

There is an increasing demand for steam power plants to operate in super-critical conditions i.e. temperatures in excess of 600°C. Under these conditions creep resistant ferritic steels oxidize and therefore require coatings in order to last. Physical vapor deposition and especially High Power Impulse Magnetron Sputtering deposited CrN/NbN nano-scale multilayer coatings with a 2.45 Cr/Nb ratio showed excellent performance when exposed to 650 °C in pure steam environment up to 2,000 h. However the role of Nb in offering protection is unclear. In order to study the long term behaviour of this type of coatings as well as to determine the influence of Nb on their oxidation resistance, a CrN/NbN coating with a 1.16 Cr/Nb ratio was studied for 12,650 h. The coating is hard, well adhered and resistant to environmental corrosion, which are properties required in particular for coatings to be applied on turbine blades. The coating also protects P92 from steam oxidation at 650º C, however coating growth defects influence significantly the oxidation resistance. The long-time exposure allowed to study the protection/ degradation mechanisms provided by this type of ceramic coatings. It was found that oxide nodules grow due to the presence of coating defect originated from substrate defects. Moreover, the higher Nb CrN/NbN coating slowly oxidizes, consuming the coating to a large extent after 12,650 h. As a result, protective oxides containing Cr and Nb are developed, remaining well attached to the substrate for at least the test duration, and preventing further substrate oxidation by steam. Interestingly, thin voids present in the as deposited coating self-heal by forming Cr rich oxides, which block steam to reach the substrate.

Keywords: steam oxidation,CrN/NbN coatings, self-healing cracks, HIPIMS

1. Introduction

In order to increase the efficiency of steam powered turbines, there is a growing demand for operation under super-critical conditions i.e. temperatures in excess of 600°C and pressures higher than 280 bar. However, this demand presents a challenge for material selection as higher operating temperatures imply the use of materials with higher creep and oxidation resistance. High chromium (Cr) steel grades (9% Cr) such as P92 can be candidate materials for manufacturing turbine components provided that their adequate mechanical properties are complemented by increasing their inherent limited oxidation resistance with a protective coating [1]. Coatings and surface treatments, in particular those with high Cr content (> 12%) which are able to form dense (less porous), protective oxides of Cr (e.g. Cr_2O_3) and maintain integrity without inter diffusion of elements, especially at elevated temperatures of 600 °C and above, can thus be useful to increase the oxidation resistance of P92 [2].

In this scenario, the physical vapour deposition (PVD) coating technique can be very useful in depositing oxidation resistant coatings. This technique has the advantage that coatings of a wide variety of elements in either their pure or compound form (nitrides, carbides, oxides or combination of all these) can be deposited. With the introduction of the novel High Power Impulse Magnetron Sputtering (HIPIMS) technique, very dense coatings with high adhesion can be deposited [3] which can address the requirements of oxidation resistant surface layers. Recently, the behaviour of such PVD coatings for steam turbine components has been explored [4, 5]. Metal nitrides were chosen due to their hardness as steam turbine blades can be exposed to erosion from, for instance, spalled oxides, coming from the boiler and/or any other component located up-stream.

Nanoscale multilayer PVD coatings have several advantages over monolithic (single layer) coatings. In depositing multilayer coatings, their microstructure is manipulated, wherein several interfaces within these coatings are intentionally created by depositing alternate layers of different composition materials. This also gives an opportunity to combine inherent properties of the individual layers into a single coating. PVD and especially HIPIMS deposited CrN/NbN nanoscale multilayer coatings have exhibited excellent room temperature wet corrosion resistance, wear resistance [6, 7] and tribo-corrosion resistance [8, 9]. In this case, inherent hardness of CrN and NbN is combined with the higher electrochemical

2

resistance of NbN resulting in a coating with a superior wear resistance and corrosion resistance [6]. Moreover the coatings were also found to possess superior oxidation resistance (air) up to a temperature range of 820 - 850 °C depending on the stoichiometry of the coatings (N/Me ratio) [10, 11]. Literature suggests that the oxidation behaviour of Nb is very complex. It can provide some oxidation resistance (in the temperature range of 600 -1000 °C) mainly because of its refractory nature [12, 13], provided that the oxide scales (Nb_2O_5) remain attached to the substrate or are less porous in nature [14-17].

There are few studies regarding the oxidation behaviour of Nb containing nitrides. For instance, Z. Qi and co-workers found that magnetron sputtered NbN and NbN_2 oxidized under air at 350-500° C forming a Nb_2O_5 thin layer that exhibited cracks and pores. On the other hand, finely grained NbN_2 exhibited lower oxidation rates and this was attributed to finer columns present in NbN_2, which in turn produced finer grain Nb_2O_5 columns, which can accommodate higher critical compressive stress without cracking [18]. In another study, HIPIMS deposited CrN/NbN multilayer coatings showed excellent performance when exposed to 650 °C in a pure steam environment [4]. This coating exhibits a nanoscale multilayer very different from the typical columnar grown films produced by sputtering. The coating composition mainly consisted of a higher atomic % of Cr as compared to Nb (N: Cr: Nb = 58.0: 29.9: 12.2 at. %), and the coated substrates (P92) exhibited two orders of magnitude less weight gain as compared to uncoated substrates after 2,000 hours of testing. It is clear that a CrN/NbN coating provides good protection under these conditions. However the role of Nb in offering protection is unclear. Another study was conducted with a coating with twice the Nb content (N: Cr: Nb = 51.4: 26.2: 22.5 at. %), and up to 2,000 h the coating exhibited a slightly higher oxidation rate for a similar surface finished substrate [5]. In any case, the oxide developed on the coating was too thin to be studied and the mechanisms of protection/degradation of the coating could not be studied. Thus, in order to determine the influence of Nb on the long term oxidation resistance and on the protective oxide formed on these coatings, as well as to establish the protection/degradation mechanisms, a CrN/NbN coatings with higher Nb content, deposited by the HIPIMS technique were studied for significantly longer exposure.

It is clear that a CrN/NbN coating provides good protection under these conditions. However the role of Nb in offering protection is unclear. Another study was conducted with a coating with twice the Nb content (N: Cr: Nb = 51.4: 26.2: 22.5 at. %), and up to 2,000 h the coating exhibited a slightly higher oxidation rate for a similar surface finished substrate [5]. In any

case, the oxide developed on the coating was too thin to be studied and the mechanisms of protection/degradation of the coating could not be studied. Thus, in order to determine the influence of Nb on the long term oxidation resistance and on the protective oxide formed on these coatings, as well as to establish the protection/degradation mechanisms, a CrN/NbN coatings with higher Nb content, deposited by the HIPIMS technique were studied for significantly longer exposure.

2. Experimental details

2.1 Coating deposition

Nanoscale multilayer CrN/NbN coatings have been deposited in a conventional industrial Unbalanced Magnetron Sputtering (UBM) machine (HTC 1000-4, four-target system (Hauzer Techno Coatings, Europe B.V., Venlo, The Netherlands) on P92. In this machine, coatings can be deposited either by UBM or HIPIMS or a combination of both techniques depending on the requirements. For this study, coatings were deposited with 2 cathodes powered by HIPIMS (Hüttinger Elektronik Sp. z o.o., Warsaw, Poland) and 2 cathodes powered by d.c. magnetron power supplies. Details of the machine such as arrangements of the targets, substrate holder and coating details (multilayer coating scheme) can be found in previous publications [4, 7].

For oxidation studies coatings were deposited on ground P92 steel specimens with a surface finish with deep grinding marks (Ra: 0.63 µm). Subsequently, all the coupons were subjected to a 3 step sequence of an adhesion enhancing HIPIMS Cr ion etching [19], followed by a CrN base layer deposition and bulk coating deposition consisting of alternating nanoscale CrN and NbN layers.

2.2 Coating characterisation:

In order to investigate their performance, the coatings were characterised using a number of analytical techniques. Scanning Electron Microscopy (FEI NOVA-NANOSEM 200 and Zeiss Supra 55VP, Focussed Ion Beam SEM (Quanta 200 3D) were used to analyse the coating microstructures. XRD was carried out by means of a Philips X`Pert using the Cu Kα line (0.154 nm).

Coating adhesion was measured by progressive loading scratch test conducted on CSEM-Anton Paar REVETEST device. The coating hardness was measured by the Knoop method with a MITUTOYO microhardness tester using normal load of 25 g, (approx.0.25N).

2.3. Steam oxidation test

P92 uncoated substrates were ground (Struers 120) prior to testing whereas the coated specimens were tested as coated. The schematics of the closed loop laboratory rig employed at INTA is shown elsewhere [20]. Prior to testing, laboratory air was displaced from the specimen chamber by means of N_2 which was kept flowing while heating up to the test temperature (approximately at a rate of 600º C/h). Once the test temperature was reached, the N_2 flow was stopped and pure steam was introduced at a linear velocity of 8 cm.s^{-1}. To carry out weight measurements or to remove samples, the furnace was cooled to about 300º C under N_2 atmosphere and the specimens were subsequently removed. The reheat cycle was also carried out under N_2 atmosphere.

The oxidation kinetics were evaluated by mass gain measurements in a four decimal balance. The specimens were removed from the chamber at fixed intervals. Spalled oxides if any, were not included during the weighting process.

3. Results and discussion:

3.1 Coating mechanical properties and adhesion

High hardness values exceeding $HK_{0.25N} = 3300$ were measured due to the special layered coating structure on nanoscale. Owing to the surface pre-treatment with HIPIMS technology by which prior to the coating deposition, the substrate is bombarded with accelerated metal ions, high adhesion critical load values of $L_C = 80N$ were measured for CrN/NbN deposited on P92 steel. Detailed information about the fundamentals and the technological parameters of the surface pre-treatment process can be found elsewhere in [3].

3.2 Coating morphology

Detailed SEM analysis on the high Nb content coatings deposited on P92 samples showed the coating to be very dense in spite of the surface being very rough. Figure 1 (a-d) shows the SEM images obtained in secondary electron imaging mode. Figure 1a shows the overall surface of the coated P92 specimen in a low magnification. PVD coatings, being thin in nature and a line of sight process, replicate the surface topography, in this case the grooved topology of the substrate caused by grinding. The coating appears very dense with uniform coverage as evident in figures 1c and d due to the persistent and intentional ion bombardment of the depositing species (as a result of the higher ion to neutral ratio of the depositing flux) obtained in a HIPIMS plasma, leading to a higher ad-atom movement before they condense in a

growing film. On the surface image (figures 1a and b) both grinding marks and growth defects can be observed, and as shown on the cross section image (figure 1c), the growth defects appear to be associated with the "hills" produced by grinding. These growth defects are typical of PVD coatings and in the present coating, they appear quite frequently. No cracks could be observed from the surface. Dense, very fine-grained-dome columnar shaped grains growing adjacent to each other to form the bulk coating. This coating micro-structure, typically obtained by a combined process of HIPIMS and Unbalanced Magnetron Sputtering (UBM) techniques [4, 6] is also evident in the higher magnification SEM images shown on figure 1b. Finer grain size in a PVD coating indicates higher nucleation rates thus leading to denser coating, which is paramount to protect the substrate. The true nature of the 3.5 µm coating density and specimen coverage, is however more evident in the cross-sectional image, figure 1d, obtained by the Focussed-Ion-Beam (FIB) technique. Yet, some voids can also be observed in the as deposited coating, again generally associated with substrate irregularities as seen in figure 1c. A cross-sectional TEM image showing multilayer arrangement in a typical CrN/NbN PVD coating can be seen in one of the previous publication [7].
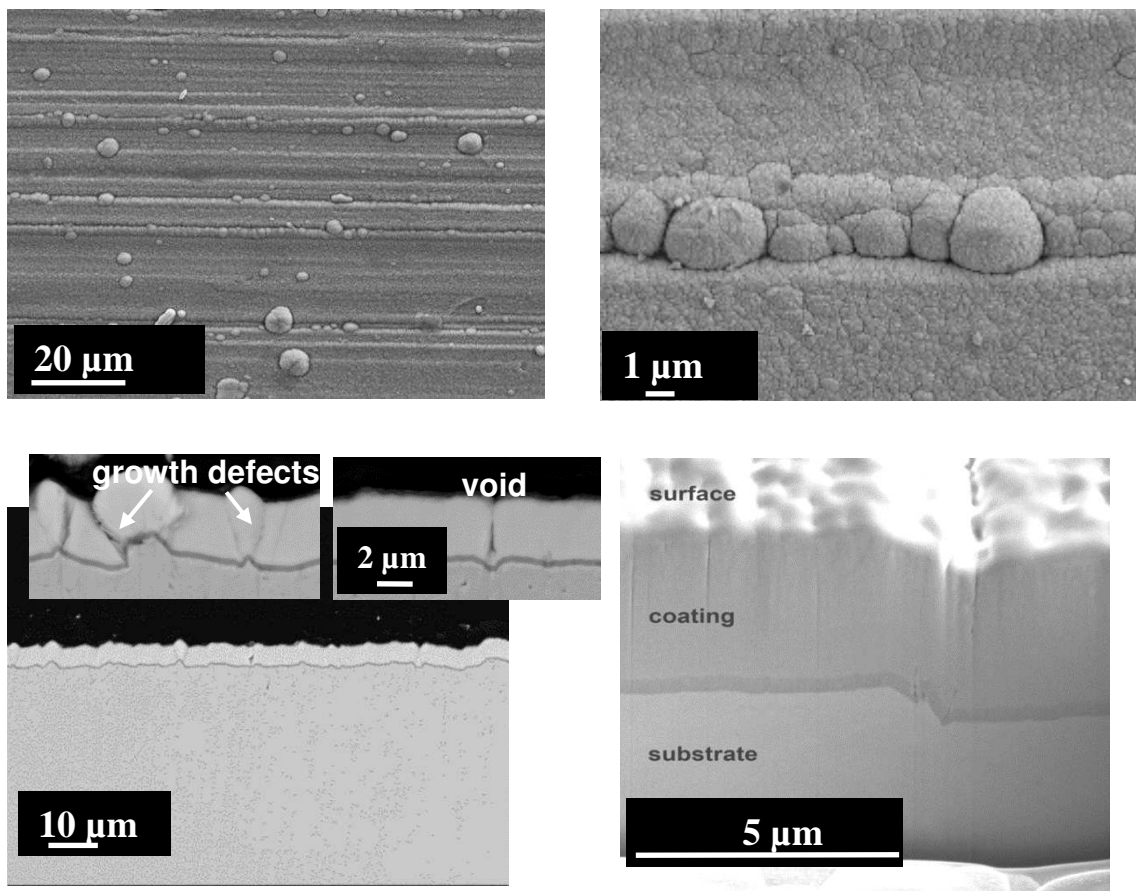

Figure 1: Scanning electron microscope images of CrN/NbN coating on P92 substrate: (a) surface image at low magnification (b) surface image at a higher magnification (c) cross-section and d) FIB cross-section image at a higher magnification.

6

As deposited CrN/NbN coating consists of CrN and NbN layers deposited on top of each other in which the metal nitride is an interstitial compound of either Cr or Nb and nitrogen [4]. XRD measurements revealed that the coating has a NaCl type face centred cubic (f.c.c) structure as shown in figure 2. The XRD pattern is typical for multilayer coatings where only one peak appears located in the middle of the reflections as a weighted mean of the individual reflections from CrN and NbN. As evident from the figure, the coating has a (111) and (200) preferred orientation.
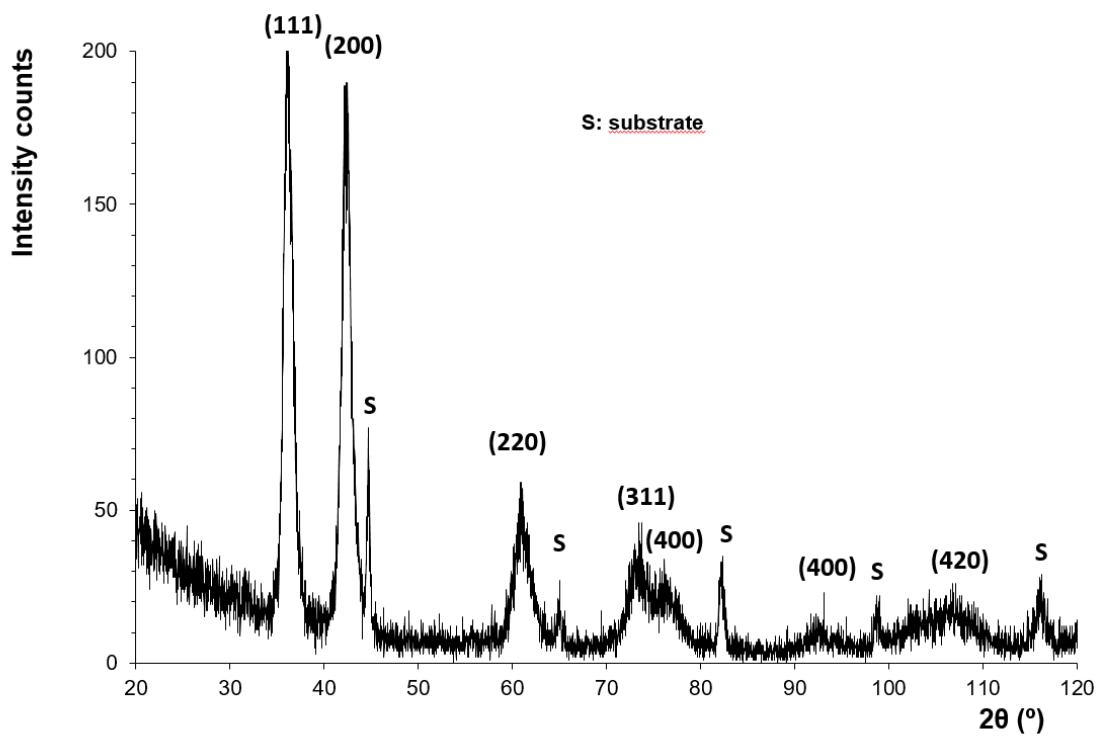

Figure 2: XRD of 'as deposited' CrN/NbN

3.3 Steam Oxidation Behaviour

CrN/NbN coated P92 substrates were subjected to oxidation tests at 650 °C for up to 12,650 h in a pure flowing steam environment. Figure 3 shows the weight variation of both coated and uncoated P92 (for comparison purposes).
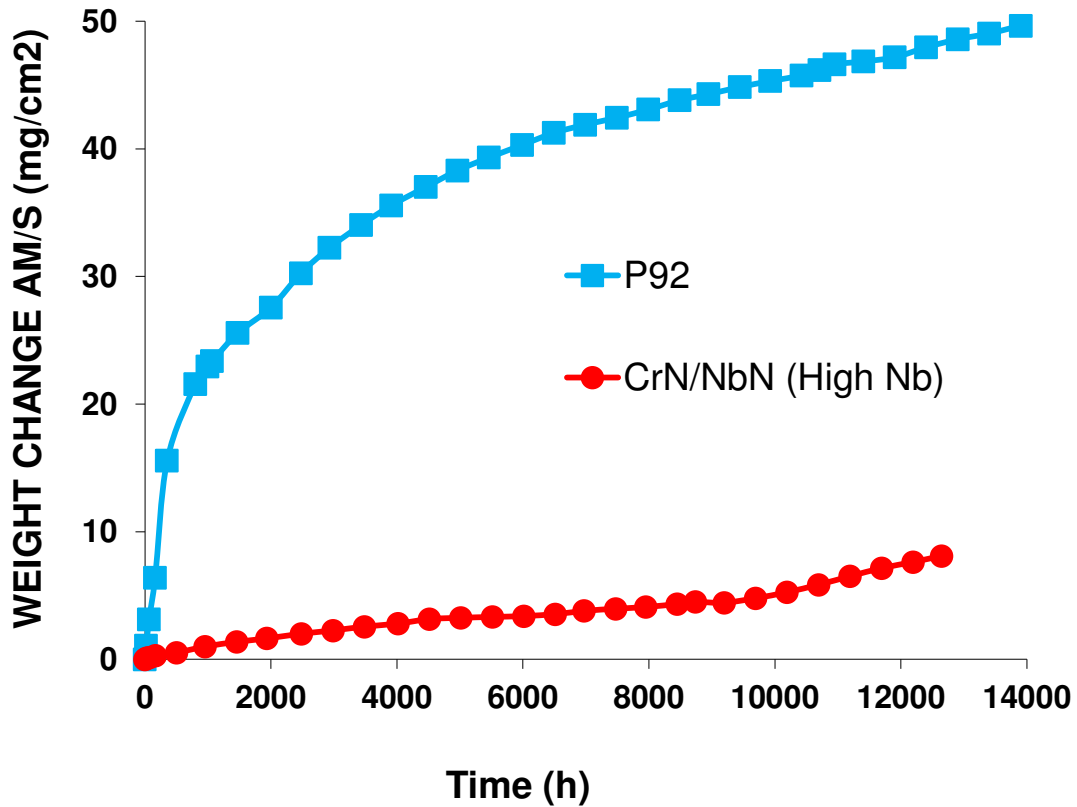
Figure 3: Mass variation of CrN/NbN coated and uncoated P92 as a function of exposure time under pure flowing steam at 650°C

As observed, CrN/NbN coated P92 begins by exhibiting a low mass gain as compared to the uncoated substrate, which is known to develop thick oxide scales after short exposures [19, 21]. However, after $\approx$ 8,000-9,000 h the oxidation rate of the coated sample increases and the slope of the weight variation curve becomes similar to that of uncoated P92 after the same exposure. When comparing the higher Cr containing coating tested during our previous study [4] with the present higher Nb one, the initial oxidation rates of the latter is a bit lower at the initial stages. However, after approximately 800 h the higher Nb coating exhibits higher oxidation rates, as shown in figure 4 on which the weight variation data obtained for both coatings are compared. These may indicate that the initial protective oxide is formed faster on the higher Cr coatings. In contrast, on the higher Nb layers, once developed, the oxide grows faster, which determines the long term protective behaviour of these coatings.
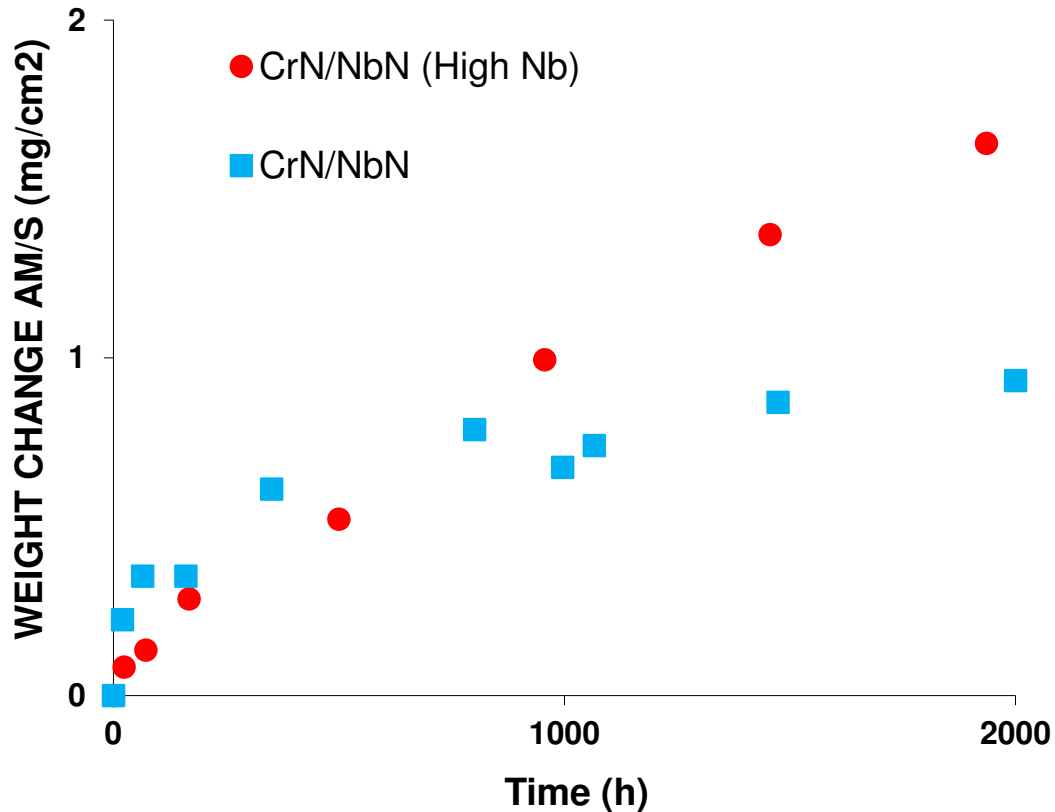
Figure 4: Comparison of the mass variation of CrN/NbN coatings with high (present work) and low Nb (from [4]) as a function of exposure time under pure flowing steam at 650°C.

Figure 5 shows the surface of the coated samples exposed to steam after 3,500 and 7,900 h. On the 3,500 h sample, large nodules can be observed, which become even larger and more abundant on the 7,900 h sample. On the specimen exposed to 12,650 h further growth of the oxide nodules is observed on its surface. Mapping of a nodule found on the 3,500 h sample shows that it corresponds to Fe oxide whereas the surface of the coating is covered with Cr and Nb rich oxides (figure 5c). Surface EDS analysis of the nodules indicated that only Fe (39.9 at. %) and O (60.1 at. %) are present and that the relative content evidences that it corresponds to Fe_2O_3. The high coverage of the surface by Fe oxide nodules observed in the sample exposed for 7,900 h may explain the increase in the slope of the weight variation vs time curve (figure 3). Fe rich oxides grow faster than Cr rich oxides and the observed slope similarity with that of the uncoated substrate appear to justify this hypothesis.
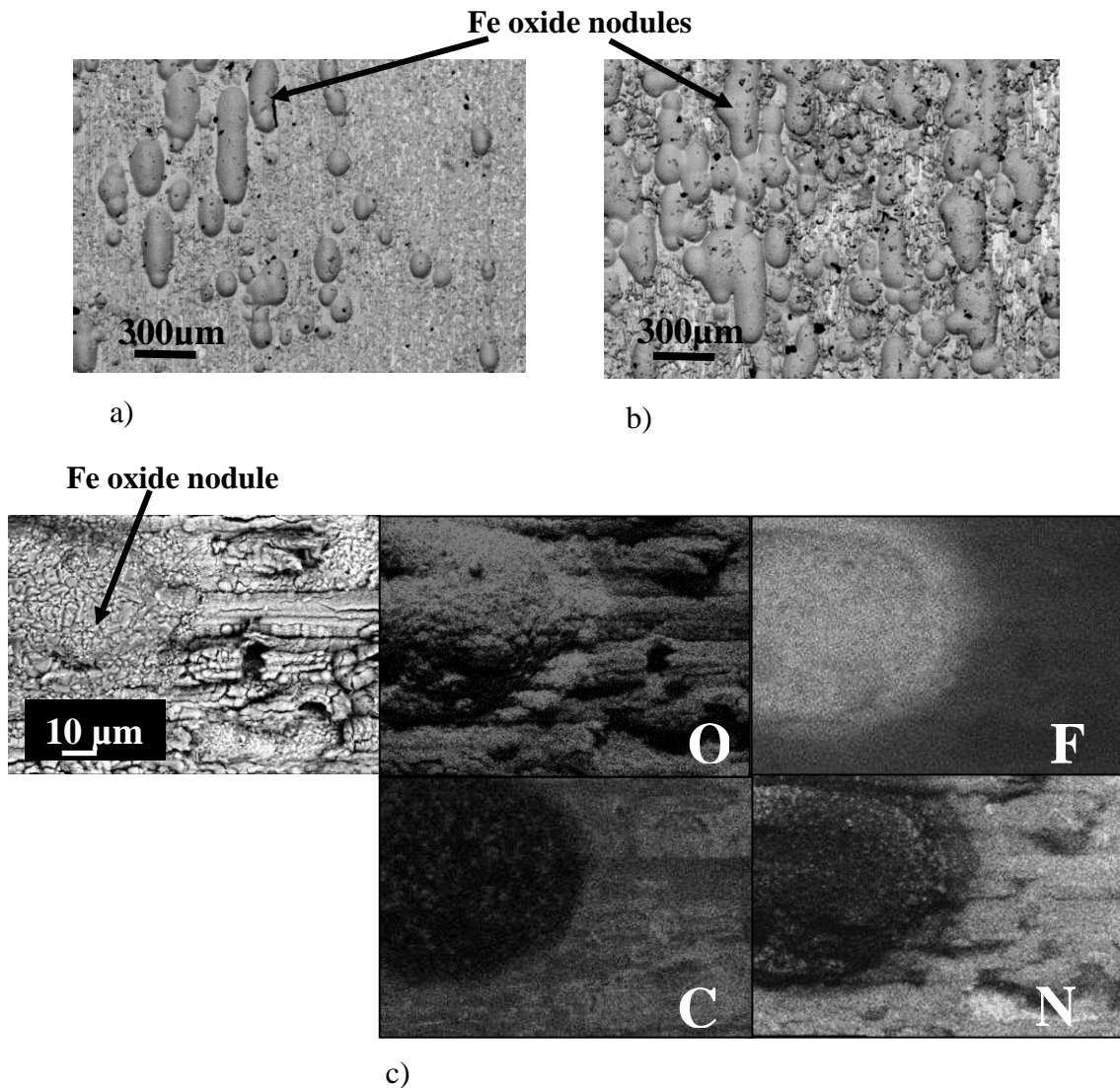
Figure 5: CrN/NbN coating exposed to pure flowing steam at 650° C: a) surface image after 3,500 h, b) surface image after 7,900 h and c) EDS element mapping of a nodule and its surroundings found on the specimen taken after 3,500 h.

On the cross section image of the sample exposed for 3,500 h shown in figure 6, it can be clearly seen how the oxide nodules originate from local zones that perhaps resulted from the detachment of coating growth defects present in the "as deposited" coating. Indeed, not many growth defects were left in the exposed samples, whereas the "as deposited" coating exhibited a relatively large number as discussed in previous paragraphs. This can be indicative that the original coating growth defects may be weak points, as they could detach from the coating due to thermal stresses during heating and/or cooling, right at the beginning of the test, leaving the substrate exposed to steam, so that oxidation would begin immediately. Alternatively, steam could reach the substrate via the growth defect boundaries, resulting in substrate oxidation and growth defect detachment. The substrate corrosion products grow out through the defect, "overflowing" on top of the coating and undercutting below it, therefore

generating the observed oxide nodules. In agreement with these results and our corresponding interpretation, Illana et al [4] found that a smoother surface finish without so many grinding marks, resulted in a lower oxidation rate due to the reduced coating growth defect density. As already shown in the previous paragraphs, the coating growth defects appear to originate mostly on the grinding marks.
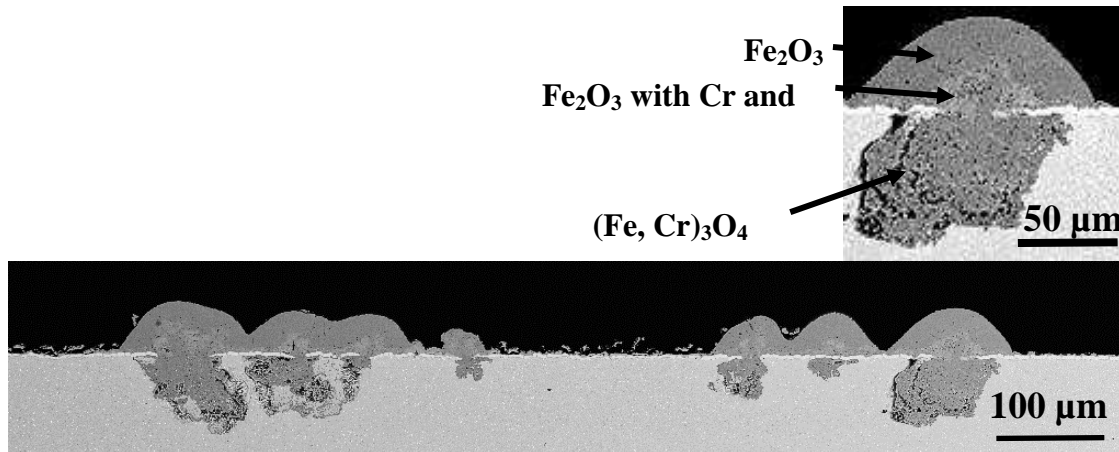

Figure 6: SEM cross of CrN/NbN exposed to pure flowing steam at 650°C after 3,500 h.

Away from the centre of the nodule (likely where it originated), but still within it, the coating remains attached to the original surface, right between the outer and inner growing oxides as shown in figure 6. The observed outer, darker zone of the oxide is indeed Fe_2O_3. Under it, and on top of the centre of the nodules, a lighter intermediate zone can be observed (figure 6). EDS analysis showed that other than Fe and O, it also contains Cr (5.1 at. %) and Nb (5.5 at. %), indicating interdiffusion/reaction of the coating elements with the Fe oxide which grows through the defect, as can be seen in the corresponding element map on figure 7.
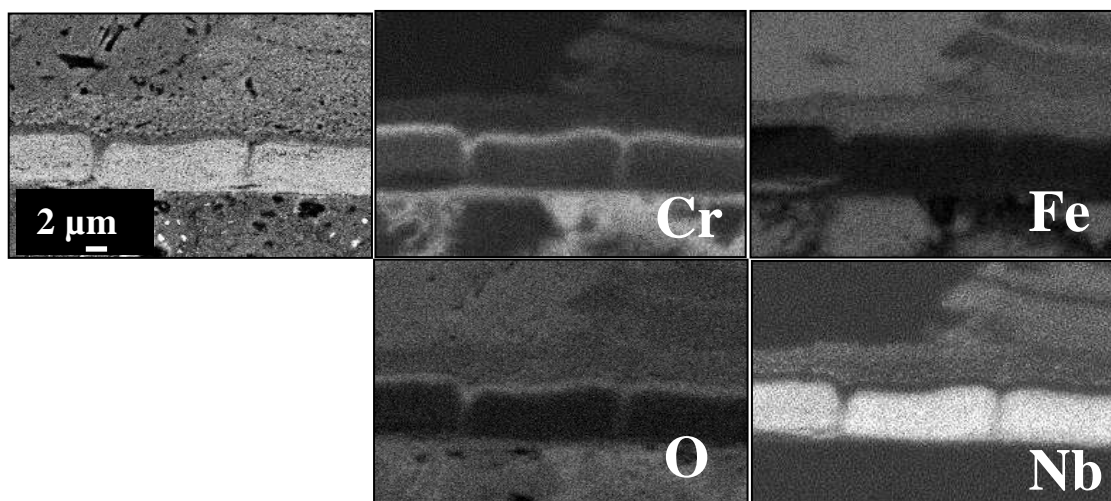
Figure 7: Element EDS mapping of CrN/NbN exposed to pure flowing steam at 650°C after 3,500 h at a zone were the oxide nodule had grown both on top and below of the coating .

Ferritic steels exposed to pure flowing steam at temperatures higher than 550° C usually develop Fe_3O_4, which appear to be more stable than Fe_2O_3 under said conditions [21]. In the present case, the presence of the coating seems to somewhat hinder Fe outwards diffusion, and therefore Fe_2O_3 is the major external oxide. The oxide present within the substrate and under the coating, contains principally Fe (29.0-32.0 at. %) and Cr (8.0-12.0 at. %) as well as other elements present in the substrate such as W and Mn, but in very small amounts (not shown in the element map). Likely, this inwards growing oxide is a Fe, Cr spinel typically formed on ferritic steels when exposed to steam at high temperature [21]. The CrN/NbN coating located under the overflown oxide maintains the as deposited thickness and does not contain Fe in significant amounts. A thin oxide ($\approx$ 0.8 µm) rich in Cr (34.6 wt. %) with minor amounts of Nb (6.9 at. %) and some Fe (4-9 at. %) has developed on its surface. Cr is known to be a protective oxide former so this is not surprising, and the presence of Fe can be explained by interdiffusion with Fe_2O_3 laying right on top, as the nitride coating has no Fe. As already mentioned, Cr and Nb also diffuse outwards enriching Fe_2O_3 in these two elements.

On the other hand, the coating present in zones on which there is no nodules and substrate corrosion (and it is therefore not covered by Fe_2O_3), has lost some thickness and the protective oxide covering its surface is significantly thicker than that observed under the substrate corrosion products within the observed oxide nodules. Said oxide reaches up to 3 µm as seen in figure 8a. The coating composition has changed (N: Cr: Nb: O = 48.5: 21.6: 24.7: 3.5 at. %) as the Cr/Nb has decreased from initially 1.16 to 0.87 indicating Cr loss.

Some oxygen has diffused into it, as well as some Fe (> 1 at. %) perhaps due to some inter-columnar oxidation and diffusion respectively. The very high magnification image of the coating shown in figure 8b supports this interpretation, as cracks/voids and column boundaries appear oxidized. Interestingly, said cracks/voids or boundaries self-heal and do not appear to cause substrate oxidation. The oxide developed on top of the nitride coating has variable composition: it is rich in Cr (Cr: Nb: O: Fe:= 21.8: 7.7: 68.6: 1.9 at. %) on areas close to the coating interface, whereas at the outer most zones, it is significantly poorer in Cr and richer in Nb and Fe (Cr: Nb: O: Fe: = 10.0: 9.9: 71.6: 7.7 at. %). The presence of Fe in this oxide is puzzling, but could perhaps result from lateral diffusion coming from the Fe oxide nodules located nearby.
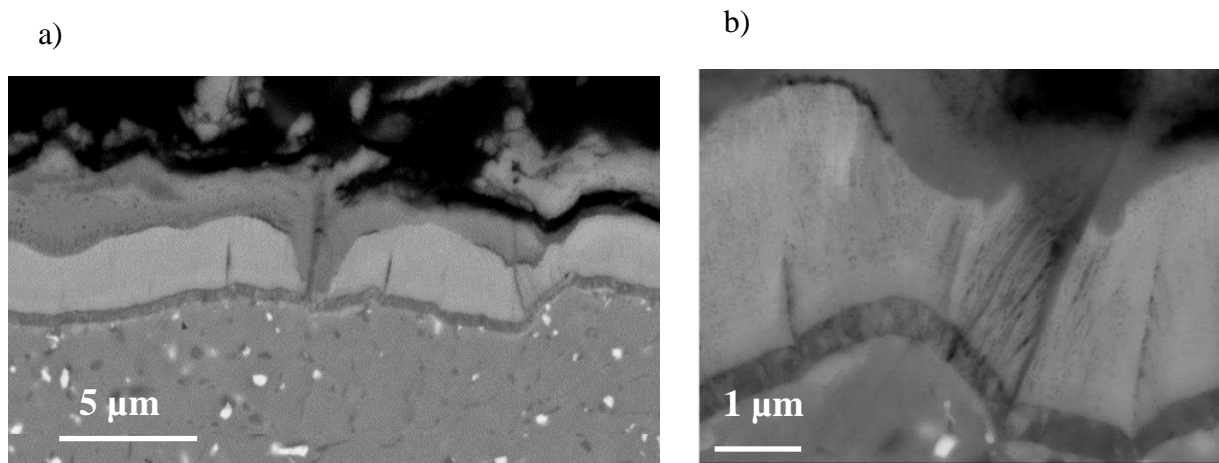
a) b)

Figure 8: a) Cross-section of CrN/NbN exposed to pure flowing steam at 650°C after 3,500 h at a zone where there is no substrate corrosion products and b) higher magnification showing inter-columnar oxidation

Depletion of Cr at the coating surface, takes place as observed in the element mapping shown in figure 9, and it is also confirmed by dot EDS analysis which indicates a content of Cr as low as 10 at. % right at the interface with the oxide, whereas within the bulk, the content is of 22 at. %. In contrast hardly any Nb depletion is observed. On specific less abundant spots, the CrN/NbN coating has totally oxidised (figure 8a), but the oxidation does not extent into the substrate as it appears to be stopped by the very thin base CrN layer still located at the original substrate coating interface.
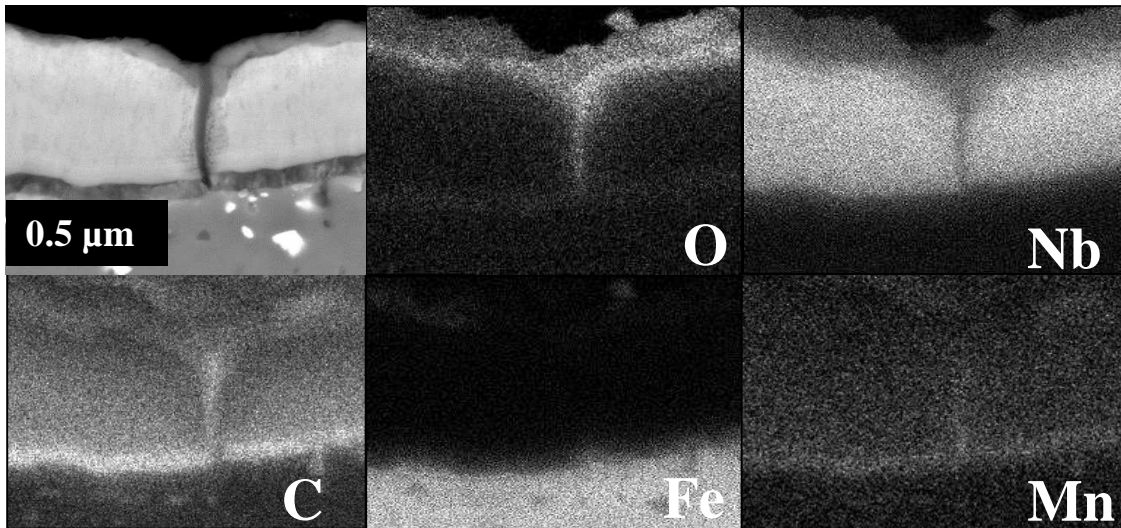
Figure 9: Element EDS mapping of CrN/NbN exposed to pure flowing steam at 650°C after 3,500 h at a zone where there is no substrate corrosion products.

As already mentioned, thin cracks/voids filled with a darker looking oxide can be frequently observed, most of them reaching the substrate, pass the CrN base layer, but without penetrating it. These self-healing cracks are filled with oxides containing Cr, Nb, Mn and some Fe, as seen in the map shown in figure 9. Indeed, some Mn coming from the substrate can be observed at the base of the filled voids indicating that the healing mechanism not only takes place by protective oxide formed on the surface of the void, but also from Cr (and Mn) diffusion from the substrate. The thin crack/void self-healing process must have taken place very fast no evidence of substrate oxidation can be found as under it.
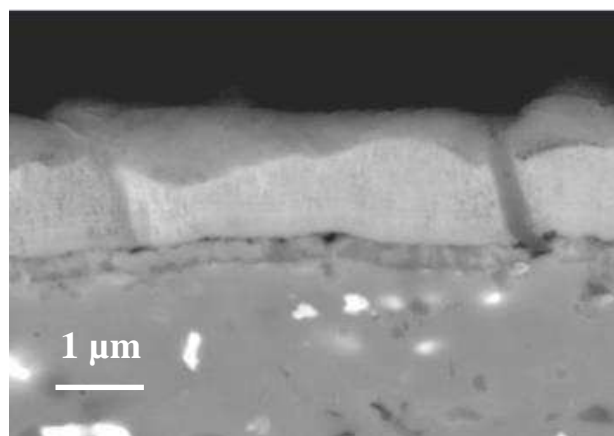

Figure 10: Cross-section of CrN/NbN exposed to pure flowing steam at 650° C after 7,900 h at a zones where there is no substrate corrosion products.

After 7,900 h the oxidation process continues, resulting in larger nodules of substrate corrosion products, as well as in further coating oxidation as seen in figure 10. Less than 1.5 μm of coating is left in some areas. The oxide developed by the coating is nevertheless protective when compared to Fe oxides and Fe, Cr spinels formed by the substrate. XRD of this specimens show mainly peaks attributed to Fe_2O_3 but some peaks with lower intensity correspond to Cr_2O_3 and two others at approximately 22 and 27º, also with low intensity, could be assigned to Nb_2O_5, the most common of the Nb oxides (figure 11). In the published literature, no mention of mixed Cr, Nb oxides could be found. This observation contrasts with our prior study, in which peaks that could only be attributed to NbO were found.
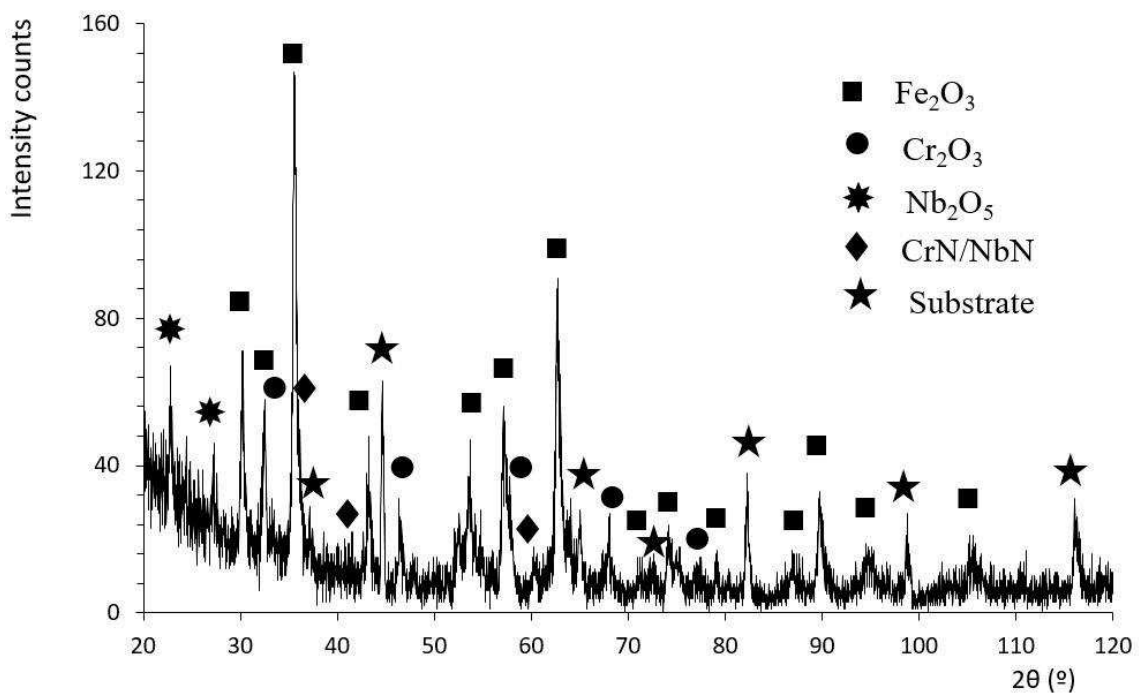

Figure 11: XRD of CrN/NbN exposed to pure flowing steam at 650ºC after 7,900 h

The coating has lost more Cr as its Cr/Nb ratio continues to decrease (0.75), whereas the oxygen content within the coating has increased to an average of 15 at. %. In addition, Fe and Mn have diffused into the coating and average contents of 3.5 and 2.1 at. % respectively, could be measured. As in the 3,500 h samples, thin cracks filled with oxide rich in Cr and Mn (coming obviously from the substrate beneath the crack tip) are present, therefore healing the coating and preventing the substrate to be attacked by steam.

Coating oxidation proceeds and after 12,650 h, most of the coating has disappeared on the areas that remain uncovered by oxide nodules (12a) and even in areas "protected" by Fe_2O_3 most of the coating has also oxidised as seen in figure 12b.
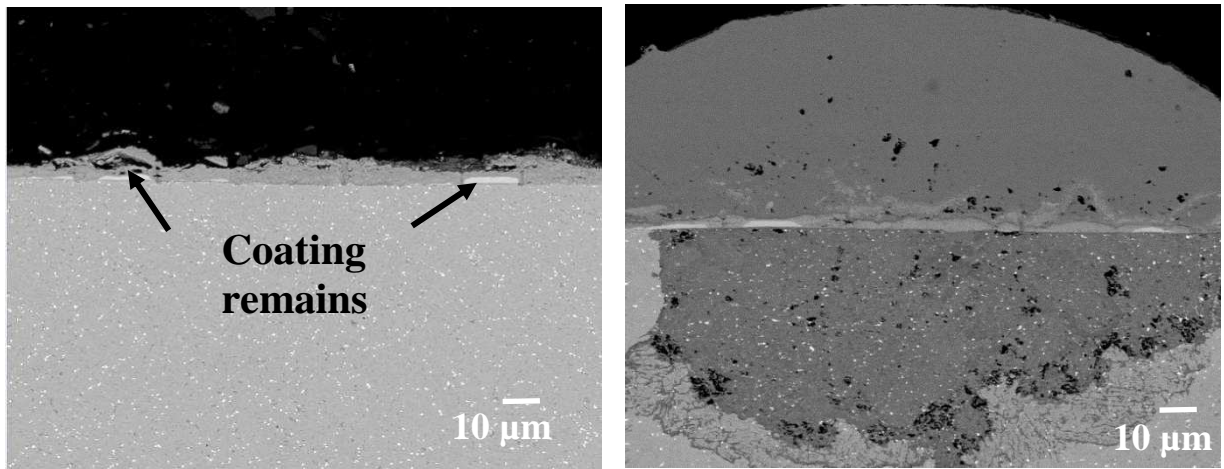

Figure 12: Cross-sections of CrN/NbN exposed to pure flowing steam at 650°C after 12,650 h at zones without (a) and with (b) substrate corrosion products.

The oxide produced by this coating has higher volume than the corresponding nitride as it has reached 10 to 15 µm indicated by the Pilling-Bedworth ratio between the oxide and coating volume. This is not unexpected as according to Kidszum et al [22], the Pilling-Bedworth ratio for NbN was calculated to be 2.35 for Nb_2O_5 as oxide. In the present case the oxide scale exhibits a complex morphology, likely indicating that it is rather a mixture of more than one oxide as shown in figure 13, and the presence of Cr, as well pores and inter-oxide detachment can cause an even higher apparent ratio. The base CrN layer under the CrN/NbN coating has been significantly enriched in Fe (16-30 at. %) and the remaining oxide has an even lower Cr/Nb ratio (0.68) with similar levels of oxygen, Fe and Mn as those observed in the 7,900 h, sample perhaps indicating saturation. In figure 13, immediately to the right of the remaining coating, a darker colour oxide penetrating the substrate can be observed. Said feature is reminiscent of an oxide self-healed crack such as the ones shown on figures 9 and 10.
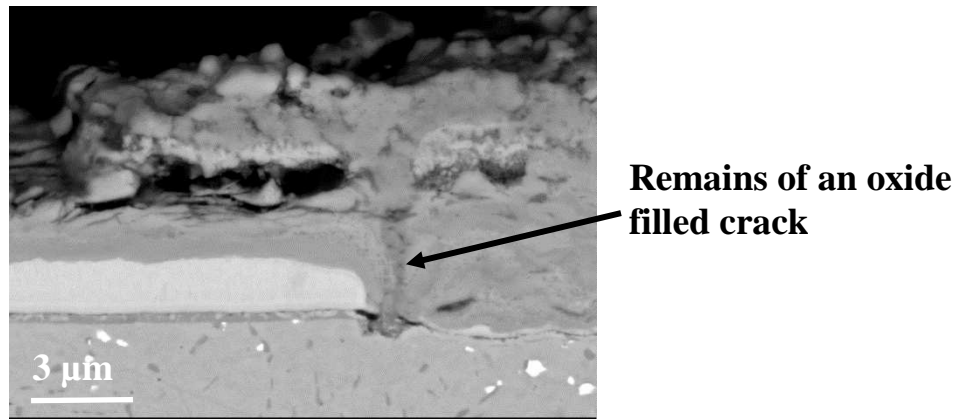
Figure 13: Cross-sections of CrN/NbN exposed to pure flowing steam at 650°C after 12,650 h at a zones substrate corrosion products.

This darker oxide is rich in Cr, has little Fe or Nb but contains Mn as shown in figure 14 on which the element mapping is presented. Cr, Mn, Fe spinels are known to be protective in particular, if they are rich in Cr and Mn [23, 24]. In the present case, this oxide formed on the lateral surfaces of the crack/void could have been further enriched with Cr by diffusion from the substrate. These observations indicate that thin voids/cracks present in the as deposited coating, or developed during heating-cooling cycles, do not necessarily lead to substrate attack and therefore, the oxide nodules observed after 3,500 h may not result from cracks/voids but rather from detached coating growth defects, which leave relatively large substrate zones exposed to steam.
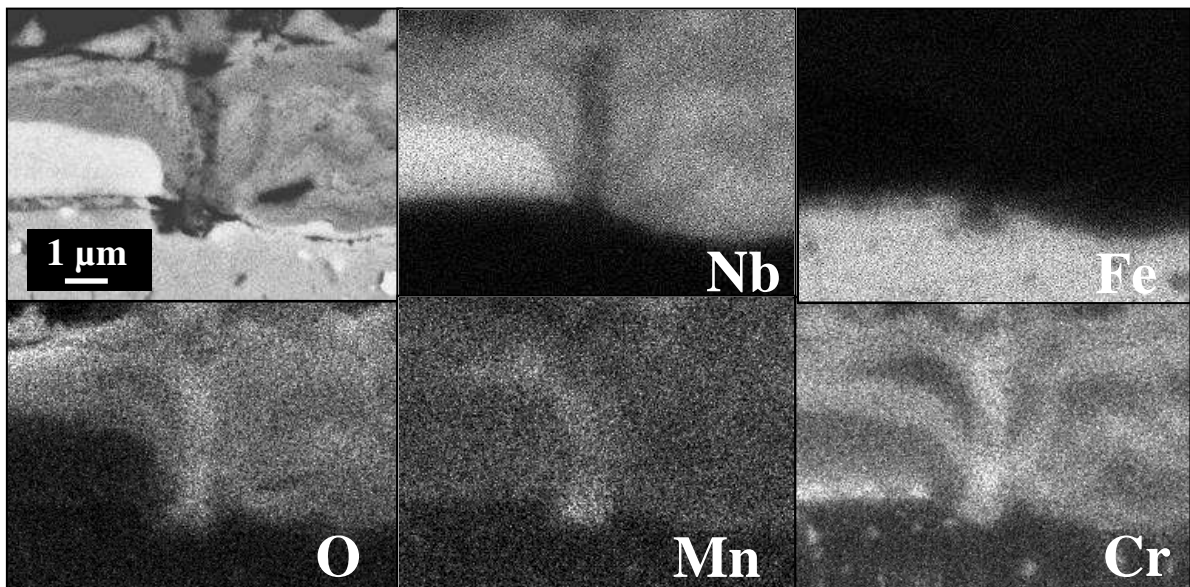

Figure 14: Element EDS map of CrN/NbN exposed to pure flowing steam at 650°C after 12,650 h.

The element map shown on figure 14 also shows a non-homogeneous distribution of Cr and Nb within the surface oxide, supporting the hypothesis that the oxide formed on top of the CrN/NbN coating is mixed rather than a complex oxide containing Cr and Nb. Further investigations including electron diffraction in the TEM are required to elucidate its microstructure. These oxides clearly protect the substrate from steam oxidation.
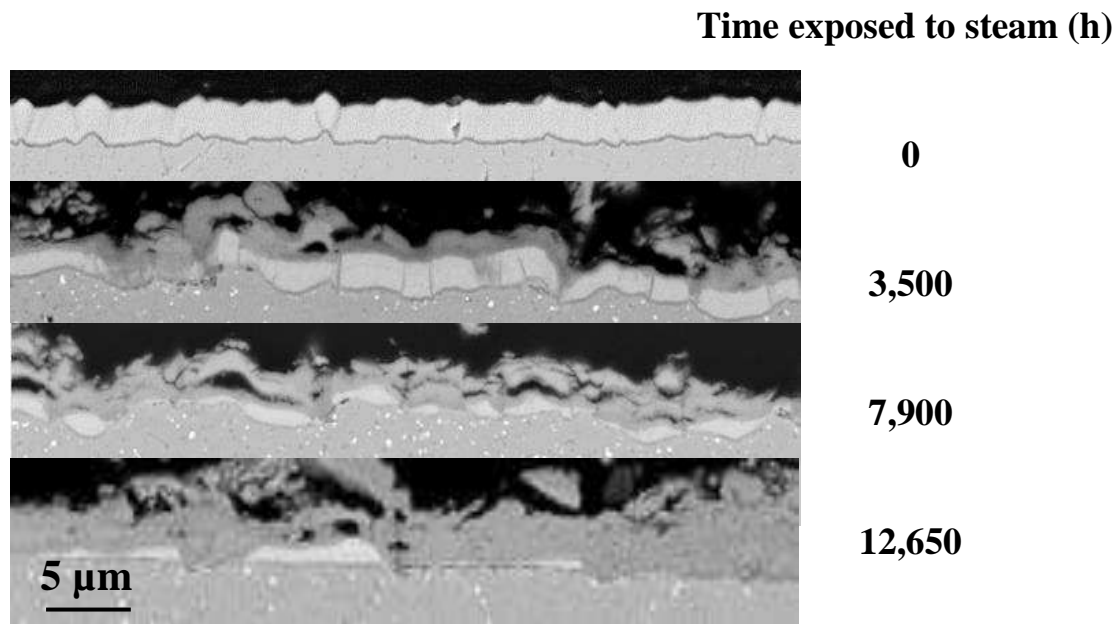
Time exposed to steam (h)

0

3,500

7,900

12,650

5 μm

Figure 15: Cross-sections of CrN/NbN exposed to pure flowing steam at 650°C as a function of exposure time. The lighter colour layer is the coating whereas the grey zones are the oxides resulting from exposure to steam

4.   Discussion

For high Nb CrN/NbN two main degradation mechanisms are suggested by the results:

1. Coating growth defects, formed due to surface imperfections may detach at the beginning of the exposure perhaps due to thermal stresses caused by heating/coolingcycles. This leads to relatively large substrate zones exposed to steam, and as the coating sides surrounding them are far apart, a self-healing mechanism is not possible. As a result, Fe_2O_3 oxide nodules form, and continue growing during exposure to steam at 650º C, both in the direction perpendicular to the substrate as well as side-ways. This observation explains the increase in the overall oxidation rate observed on the gravimetric curve shown on figure 3. If the presence of "as deposited"

coating growth defects can be avoided by preparing a smoother surface, oxide nodules could perhaps be avoided and therefore, this degradation mechanisms would disappear.

2. The main oxidation mechanism of metal nitrides is gradual replacement of nitrogen by oxygen via exchange reaction, which is due to the higher affinity of the metal for oxygen, [25]. The nitrogen atoms released during this reaction combine to form gas molecules in the surrounding atmosphere. Following this mechanism, oxidation of the coating, takes place, but at significantly slower rate than that experienced by the substrate, but nevertheless continues until all the coating is consumed. The resulting Cr and Nb rich oxide seems to be constituted by a mixture of oxides and protects the substrate from steam oxidation at least up to 12,560 h at 650º C. The behaviour of the present coating is quite better than that of pure Nb nitrides, as shown by Qi and coworkers. They found that an approximately 2 µm coating totally oxidized at 500º C after only 2 h under air [18]. Steam is significantly more corrosive than air and in the present case, it took more than 12,000 h of exposure to pure steam at 650º C to totally oxidized a 3.5 µm CrN/NbN coating likely due to the presence of Cr in the oxide and to the higher density of HIPIMS deposited coatings.

Thin through-thickness cracks may develop in the "as deposited" coating during heating due to the mismatch of the thermal expansion coefficients of the coating and substrate materials. However, these, as well as thin voids present in the "as deposited" coating (figure 1c), do not appear to become substrate corrosion pathways, as they self-heal by forming Cr rich spinels which also contain Mn, and seem to be very stable. Cr may come both from the substrate and the coating whereas Mn only from the substrate.

The coating composition evolves as it loses Cr likely because it diffuses faster than Nb, to be incorporated on the protective oxide. In parallel, O, Fe and Mn slowly incorporate in the coating likely by inter-columnar diffusion. However, the coatings appear to saturate as the content of O, Fe and Mn do not increase after 7,900 h of exposure:

h of exposure to steam at 650º C:	0	3,500	7,900	12,650
Cr/Nb:	1.16	0.87	0.75	0.68
O (at. %)	0	3.5	15	14.2
Fe	0	< 1	3	2.8
Mn	0	0	2.2	2.0

Although protective, the oxide formed on the CrN/NbN coating grows relatively fast, but even after all of the coating has disappeared, said oxide prevents further substrate oxidation at least up to 12,650 h of exposure. Almost no nitride coating is left as oxidation proceeds, as seen on figure 15 where low magnification images of the coating as a function of exposure to steam at 650º C are compared.

The results of this work also evidence that steam oxidation testing in the laboratory requires long exposures. Ilana et al tested the same coating under the same conditions for 2,000 h, up to which the coatings had not exhibited significant oxidation [5]. For this particular coating more

than 3,000 h were required to observe the oxidation of the coating. Moreover, the long term oxidation exposure allowed identification of the coating protection and degradation mechanisms.

Conclusions

A range of advanced surface analytical techniques and specialised high temperature steam test equipment was successfully utilised to reveal the degradation mechanism of a metal nitride based PVD coating in conditions of significantly long exposure times to a pure steam environment.

It was found that CrN/NbN with high Nb content protects P92 from steam oxidation at 650º C at the initial oxidation stages. After exposures longer than 7,900 h, coating growth defects detach and result in significant substrate oxidation. These defects appear to be mostly caused by the substrate grinding marks However, thin voids or cracks can self-heal preventing steam to reach the substrate. Thin protective Cr and Nb rich oxides develop and grow progressively as a function of exposure time, and are certainly less stable than other Cr containing oxides

such as Mn, Fe spinnels, which are known to be quite stable under the same conditions [22, 23]. Nevertheless, the results of this study show that HIPIMS deposited CrN/NbN coatings improve the oxidation resistance of the bare P92 by factor of 10 after long 12,650 hours exposure to 650°C.

Furthermore, the present results indicate that hard and adhesive nitride coatings could be very protective provided that they contain slow growing protective oxide formers such as Cr and perhaps Al and that coating growth defects are avoided by correct mechanical surface preparation.

Acknowledgements

References

[1] P. J. Ennis and W. J. Quadakkers, International Journal of Pressure Vessels and Piping. 84, 82-87 (2007).

[2] A. Agüero, Energy Materials, 3 (2008) 35- 44.

[3] A. Ehiasarian, "Fundamentals and applications of HIPIMS," in Plasma surface engineering research and its practical applications, R. Wei. Trivandrum, India, Research Signpost (2007) 35-86, ISBN 978-81-308-0257-2.

[4] P. Eh. Hovsepian a, A.P. Ehiasarian , Y.P. Purandare, B. Biswas, F.J. Perez, M.I. Lasanta, M.T. de Miguel, A. Illana, M. Juez-Lorenzo, R. Muelas, A. Agüero, Performance of HIPIMS deposited CrN/NbN nanostructured coatings exposed to 650º C in pure steam environment, Materials Chemistry and Physics 179 (2016) 110-119.

[5] A. Illana, S. Mato, A. Ehiasarian, Y. Purandare, M. I. Lasanta, M. T. de Miguel, P. Hovsepian, F. J. Perez-Trujillo, Substrate Finishing and Niobium Content Effects on the High-Temperature Corrosion Resistance in Steam Atmosphere of CrN/NbN Superlattice Coatings Deposited by PVD-HIPIMS, Published on line, DOI 10.1007/s11085-016-9701-5 (2016).

[6] P. Eh. Hovsepian, D. B. Lewis, W.-D. Münz, Recent Progress in Large Scale Manufacturing of Multilayer/Superlattice Hard Coatings, Surface and Coatings Technology, 133-134 (2000), p. 166-175.

[7] Y. P. Purandare, A. P. Ehiasarian and P. Eh. Hovsepian, J. Vac. Sci. Technol. A 26, 2, 288 (2008).

[8] M. M. Stack, Y. Purandare and P. Eh. Hovsepian, Surface and Coatings Technology. 188-189, 556 (2004).

[9] Y.P. Purandare, A.P. Ehiasarian, M.M. Stack, P.Eh. Hovsepian, CrN/NbN coatings deposited by HIPIMS: A preliminary study of erosion-corrosion performance, Surface & Coatings Technology 204 (2010) 1158-1162.

[10] P.E. Hovsepian, D.B. Lewis, W.-D. Munz, A. Rouzaud, P. Juliet, Chromium nitride/niobium nitride superlattice coatings deposited by combined cathodic-arc/unbalanced magnetron technique, Surface & Coatings Technology 116–119 (1999) 727-734.

[11] P.Eh. Hovsepian, D.B. Lewis, Q. Luo, W.-D. Münz, M. Meyer, High temperature performance of CrN/NbN superlattice coatings deposited on Ti-alloy substrates, Surface Engineering, Euromat Vol. 11 (1999) 41-46 proceedings, edited by H. Dimigen.

[12] C. Nico, T. Monteiro, M.P.F. Graça, Niobium oxides and niobates physical properties: Review and prospects, Progress in Materials Science 80 (2016) 1–37.

[13] G. L. Miller and F. G. Cox, Development of oxidation resistance of some refractory metals, J. Less-Common Metals, 2 (1960) 207- 222.

[14] R. Smith, The Development of oxidation resistant alloys, J. Less-Common Metals, 2 (1960) 191- 206.

[15] R. Smith, Oxidation mechanisms of Niobium, Tantalum, Molybdenum and Tungsten, J. Less-Common Metals, 2 (1960) 172- 180.

[16] W.M.M. Huijbregts, M.J. Brabers, Oxidation of niobium and of niobium coated with aluminium in steam-air mixtures, Proceedings S.E.R.A.I. Journee internationales d'étude sur l'óxydation des metaux. Bruxelles (1965).

[17] W. Wei, H. Wang, C. Zou , Z. Zhu, Z. Wei, Microstructure and oxidation behaviour of Nb-based multi-phase alloys, Materials and Design 46 (2013) 1–7.

[18] Z. Qi, A. Wu, D. Zhang, J. Zuo and Z. Wang, Microstructure, mechanical properties amd oxidation behaviour of sputtered NbN_x coatings, Journal of Alloys and Compounds, 675 (2016) 22-30.

[19] A.P. Ehiasarian, P.Eh. Hovsepian, W-D. Münz, Combined coating process comprising magnetic field-assisted, high-power, pulsed cathode sputtering and an unbalanced magnetron, Patent US7081186 B2 (25 Jul 2006), EP1260603 A2 (27 Nov 2002), DE10124749 A1 (28 Nov 2002).

[20] A. Agüero, V. González, M. Gutiérrez and R. Muelas, Oxidation under pure steam: Cr based protective oxides and coatings, Surface and Coatings Technology, 237 pp. 30–38 (2013).

[21] A. Agüero, V. González, M. Gutiérrez, R. Knödler, R. Muelas and S. Straub, Comparison between Field and Laboratory Steam Oxidation Testing of Aluminide Coatings on P92, Materials and Corrosion, 62 pp. 561-568 (2011).

[22] M. Kidzun, B. Holzapfel and L. Schultz, Ion-beam Assisted Deposition of Textured NbN Thin Films, Superconductivity Science and Technology, 23 025010 (2009).

[23] A. Agüero, V. González, P. Mayr and K. Spiradek-Hahn, Anomalous Steam Oxidation Behaviour of a High Strength 9 wt. % Cr Martensitic Steel, Materials Chemistry and Physics, 141 pp. 432-439 (2013).

[24] S. Leistikow, I. Wolf, H. J. Grabke, Effects of cold work on the oxidation behavior and carburization resistance of Alloy 800, Materials and Corrosion 38 pp 556–562 (1987).

[25] O. Kubaschewski, B.E. Hopkins, Oxidation of Metals and Alloys. London, BUTTERWORTHS, 1967.